RSC Advances

PAPER

View Article Online
View Journal | View Issue

Cite this: *RSC Adv.*, 2021, **11**, 12183

A cobalt complex with 2,4,6-tris(di-2-pyridylamine)-1,3,5-triazine: antiferromagnetic couple governed single-molecule-magnet behaviour†

Hang Gao, *[a] Ka Liu,[b] Jin Chang[a] and Juan Zhang[a]

Received 25th December 2020
Accepted 19th March 2021

DOI: 10.1039/d0ra10828f

rsc.li/rsc-advances

One cobalt complex with distorted trigonal antiprismatic geometry was obtained using 2,4,6-tris(di-2-pyridylamine)-1,3,5-triazine (dipyatriz) as the ligand. X-ray crystallography showed the complex possessing a pair of metal centers, had an antiferromagnetic coupling between two Co(II) ions. Further studied showed a field-induced slow relaxation under H_{dc} = 0.8 kOe. The peak of out-of-phase was observed after 1000 Hz, which exhibited a moderate slow-relaxation behaviour comparing to the magnetic couple for single Co(II) complex. This study may provide some strategies on designing new functional molecular magnetic materials with distinct magnetic properties and diverse the structures.

Introduction

Single-molecule magnets (SMMs), which can maintain the original magnetic properties at low temperature behind removing the external magnetic field, have attracted much interests due to the practical usages in high-density data storage, molecule electronics, and quantum computing.[1] The magnetic dilution studies showed that for the sake of achieving SMM behaviours, the magnetic interactions between the neighbouring molecules or the long-range ordering must be inhibited or tuned.[2] Although numerous molecules were discovered to have SMMs properties, the usage of these complexes were hampered because of the low blocking temperature (T_B) and the energy barrier (U). So far, many attempts have been made to increase the magnetization reversal barriers (U_{eff}) and blocking temperature. In brief, approaches have been made *i.e.* adjusting the coordination geometry of the complexes and to adopt appropriate counterions or solvents. The extensive development of the chemistry and materials revealed the major revelations of the fine details of energy levels and relaxation processes from the physics measurements at low temperatures. This field have widened recently through numerous observations for complexes containing one single magnetic ion which were named as the single-ion magnet (SIM).[3] Impressively, the barrier energy has increased a 100 fold to reach 330.0 K from 3.0 K, which offered a higher operating temperature above the physical barrier of liquid nitrogen (80.0 K) can reach.[4] The hysteresis width has also been extended to the practical limit. Although it appears that the magnetic lanthanide ions may have an upper hand on the late transition metal ions due to their large magnetic anisotropy and high spins as well as the unquenched orbital moments, the Co^{II} is the principal one of the d-ions to approach the qualities of the lanthanides.

So far, it has been discovered that many factors would have a significant influence on SMM behaviour of lanthanide complexed, including the local ligand field, the coordination geometry and the strength of the magnetic interaction between core sites. For the lanthanide SMMs, Shi and Wu have done frontier work on butterfly-shaped high nuclear Ln(III) clusters, which revealed the important role of disparate tetranuclear core arrangements of Dy^{IV} clusters.[5] Furthermore, self-assembly multi-core lanthanide clusters were extensively studied.[6] In recently years, discovery of the new SIMs has been extended to transition metals.[7] The mononuclear Mn(III) complex,[8] Mn(IV) nitride single molecule,[9] Cr(II) complexe,[10] mononuclear, two-coordinate or trigonal pyramidal complexes of Fe(II),[11] trigonal-planar mononuclear Fe(II) and Co(II) complexes,[12] and the monometallic Ni(II) complexes,[13] were consecutively studied. For these studied elements, the energy barrier can be described as $U = |D|S^2$ (or) $U = |D|(S^2 - 1/4)$, where S stand for the ground-state spin and D for the negative zero field splitting (ZFS) parameter. The energy barrier is the result of the combined effect of two parameters. Among all studied complexes, the cobalt system is one of the most favourable SIMs, for it both possesses high magnetic anisotropy as well as a high ground state ($S = 3/2$). Moreover, according to the basis of Kramers theorem, half-integer spin systems can be used to

[a]*College of Biomedical Engineering, Taiyuan University of Technology, Taiyuan, 030024, China. E-mail: hanggao@tyut.edu.cn*

[b]*Jingbo Biological Pharmaceutical Co., Ltd, Taiyuan 030003, China*

† Electronic supplementary information (ESI) available. CCDC 1919171. For ESI and crystallographic data in CIF or other electronic format see DOI: 10.1039/d0ra10828f

circumvent fast quantum tunnelling, which made Co the proper element in SIMs studies. According to research reported recently, the behaviour of single-molecule-magnets are not only affected by the coordination geometry, but also influenced by weak magnetic exchange (dipole interaction).[14] According to recently studies, the intramolecular interaction is essential to suppress the local quantum tunnelling of magnetization in the di-nuclear Dy(III) complexes.[15] However, whether the weak magnetic exchange between Co(II) ions could affect the behaviour of a single-molecule magnets remained unclear. Recently, Song reported the trigonal anti-prismatic Co(II) field-induced single-molecule-magnets behavior.[16] Based on this, for the purpose of exploring the properties of Co(II) complex possessing two Co(II) centers with a trigonal anti-prism (TAP) geometry, we designed a Co(II) complex with weak magnetic interaction between two Co(II) ions, using 2,4,6-tris(di-2-pyridylamine)-1,3,5-triazine (dipyatriz) as the ligand. The studied complex **1** displayed slow relaxation process. Herein, we reported the Co(II) complex **1** with a weak magnetic interaction between the two Co(II) ions and the magnetic properties of it in detail.

Experimental

All the reagents used for the experiment were obtained from commercial sources without further purification. Elemental analysis was conducted and further recorded on a PerkinElmer 240C elemental analyzer. The Fourier transform infrared spectroscopy was carried out in the range of 400–4000 cm^{-1} on a Thermo Scientific Nicolet iS10 spectrophotometer. The patterns of PXRD were recorded on Rigaku MiniFle600-C instrument with Cu Kα radiation ($\lambda = 1.54056$ Å) using a scan speed of 5° min^{-1} in the range of $2\theta = 5$–80°. A PPMS Squid VSM magnetometer was used to measure the alternating current magnetic (AC) data with the ac field set to 2 Oe, the frequencies were set in the range of 10 to 10 000 Hz during the test. A MPMS-XL7 SQUID magnetometer was used to measure the direct current magnetic (DC) data under 1.8 K and 300 K. The isothermal magnetization measurements were conducted subsections under 0 to 7 T. The experimental susceptibilities were corrected for the diamagnetisms estimated according to Pascal's constants as well as for the sample holder, through a precise calibration.

Synthesis of $[Co(dipyatriz)_2(H_2O)_2]\cdot 4ClO_4$ (1)

Dipyatriz (0.2 mmol, 0.034 g) and $CoClO_4\cdot 6H_2O$ (0.1 mmol, 0.0237 g) were added gradually to a 5 mL mixed solution (H_2O and CH_3CN 1 : 1). After slow evaporation, red crystals were obtained and carefully collected. Anal. calc. (%) for $C_{66}H_{68}Cl_4Co_2N_{24}O_{26}$: C, 42.32; H, 3.66; N, 17.95; found: C, 42.08; H, 3.92; N, 17.68; IR (ATR-FTIR, ν/cm^{-1}): 3402 (w), 3107 (w), 1609 (s), 1558 (s), 1482 (s), 1435 (s), 1403 (s), 1366 (s), 1323 (s), 1059 (s), 1020 (s).

X-ray data collection and structure refinement

A Bruker Smart CCD area-detector diffractometer was used to test the crystallographic data of the studied complex. The ω scan mode with Ga-Kα radiation ($\lambda = 1.34139$ Å) at 296.0 K was used during the test. Diffraction data were integrated with SAINT, the absorption corrections were applied with SADABS. The SHELXTL package was implied to locate the non-hydrogen atoms of the tested complex by Patterson's method, followed by difference Fourier syntheses.[17] The non-hydrogen atoms were completely refined by full-matrix least-squares on F^2. And the hydrogen bonded to carbon were determined sooner refined anisotropically. The whole calculations were conducted in the SHELXTL-97 program.[18]

Results and discussion

Crystal structures of 1

Results from the single crystal X-ray diffraction analysis demonstrated that **1** crystallized in the monoclinic, $P2_1/n$ space group. Each unit cell has a pair of Co(II) ions and ligands, six water and four ClO_4 groups. As showed in Fig. 1, the metal center Co(II) ion was six-coordinated, two Co(II) ions were lie in each end of the cell, and were bonded by four N atoms connected with ligands as well as two O atoms provided by the solvent, composing a trigonal anti-prismatic geometry. All the Co–O/N bonds in the complex were fall in the normal range. The bond length of Co–N was 2.225 Å and Co–O were 2.037 Å and 2.117 Å respectively. Two metal centers of each complex molecule were connected by two ligands forming a body structure. The details information and analysis for the studied complex as well as the crucial bond distances and angles are shown in Tables S1 and S2.†

DC magnetic measurements

The polycrystalline samples of complex **1** was used to perform the static direct current magnetic measurements. The temperature during the test was set varying from 1.8 K to 300 K under 1 kOe. As shown in Fig. 2, the $\chi_M T$ values at room temperature for **1** was 6.05 $cm^3\ mol^{-1}$ K, which was larger than the expect of 3.75

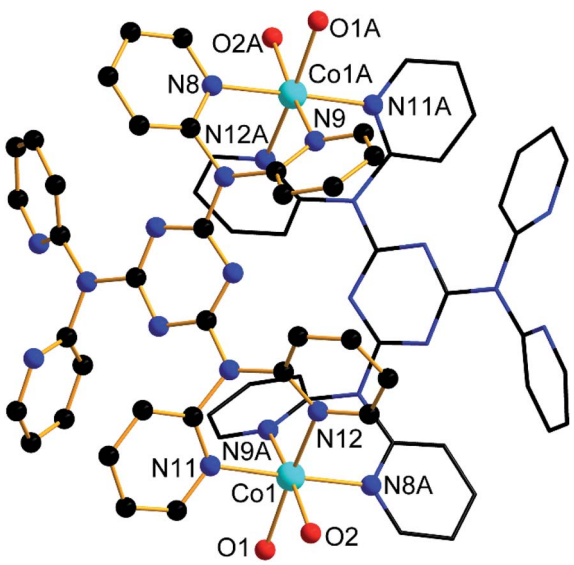

Fig. 1 Molecular structure of **1**. Only crucial atoms are labelled and the hydrogen atoms are omitted for clarity.

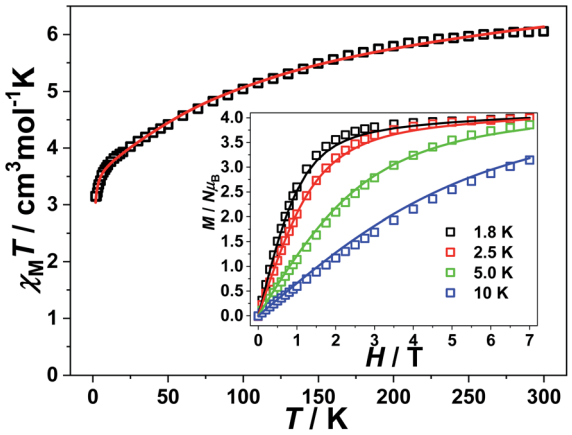

Fig. 2 Temperature dependence of the $\chi_M T$ for **1** measured at a 1.0 kOe by MPMS-XL7 SQUID. The solid red line represents the best fitting result by PHI. Inset: experimental *M vs. H* plots at different temperatures.

for two high spin Co(II) ($S = 3/2$ and $g = 2.0$). The large value suggest the existence of a strong orbital contribution to the magnetic momentum.[19] With a decrease of temperature from r.t. to 150 K, the $\chi_M T$ values were gradually decreased at the beginning, then showed a more robust decline. The ultimate $\chi_M T$ values was 3.15 cm^3 mol^{-1} K at 1.8 K. Such result is mainly caused by the intrinsic magnetic anisotropy and weak antiferromagnetic coupling between pairs of Co(II) ions. The field-dependence magnetizations of **1** were further measured at fields ranging set from 0 to 7 T with the temperature from 1.8 to 10.0 K (Fig. 2). Results showed the magnetization value under 7 T was much lower than the theoretically saturated value. In addition, the presence of strong magnetic anisotropy was testified by non-superposition of the *M vs. H*/*T* plot (Fig. 2, inset). Furthermore, to quantify the anisotropy parameters for further analysis, the PHI program was implied to fit the magnetic susceptibilities and the magnetization data of the studied complex **1**. Good result of fitting was obtained as following spin Hamiltonian.[20]

$$\hat{H} = D\left[\hat{S}_z^{\,2} - \frac{S(S+1)}{3}\right] + E\left(\hat{S}_x^{\,2} - \hat{S}_y^{\,2}\right) - 2J\hat{S}_1\hat{S}_2S_1S_2 + g\mu_B\mathrm{SH} \quad (1)$$

where D represents the axial ZFS parameter, E represents the rhombic ZFS parameter, as well as S stand for the spin projection. The best fits using PHI obtained $D = -66.88$ cm^{-1}, $E = -5.51$ cm^{-1}, $J = -0.045$ cm^{-1}, $g = 2.53$ and TIP $= 1.5 \times 10^{-4}$ for complex **1**. The distortion from the octahedral geometry of the complex may be the reason that caused the deviation of spin coupling parameter and the orbital reduction parameter. The value of negative D parameters obtained from the complex indicated that the presence of strong axial magnetic anisotropy of Co(II) in **1**.

AC magnetic measurements

Temperature and frequency dependence of the alternating current (AC) magnetic measurements were performed for the purpose of investigation the slow magnetization relaxation behavior of the studied complex on the polycrystalline samples at low temperature. Results showed no existence of the signal of out-of-phase ($\chi_{M''}$) ac susceptibility without external dc field, which may due to the efficient QTM (Fig. S1†).[21] The studied complex **1** show an obvious frequency dependence $\chi_{M''}$ in the corresponding measurements under external dc fields. Among the whole test under the dc field, the complex observed only one relaxation process.

To further study the magneto–structure correlation and the influence of packing arrangements in the crystal lattice, we chose 0.8 kOe external dc fields to test the spin relaxation behaviors.

Results showed a maximum of out-of-phase ($\chi_{M''}$) magnetic susceptibility signals can be observed with the temperature ranging from 1.8 K to 4.2 K for the complex **1** as shown in Fig. 3. CCFIT program and a modified Debye function was further used to fit the Cole–Cole plots of $\chi_{M''}$ *vs.* $\chi_{M'}$ for complex **1**.[22] The extracted α value less than 0.11 for complex **1** are shown in Fig. 4(a). In the studied complex, the α values were quite small, indicate a narrow distribution of relaxation time for the studied complex may exist.

The relaxation times τ was obtained by the fitting program and further plotted *vs.* T^{-1}, generating the Arrhenius diagram as shown in Fig. 4(b). In field-induced Co(II)-based SIMs, the multiple relaxation processes may exist. Therefore, the eqn (3) containing multi relaxation processes was used to analysis the

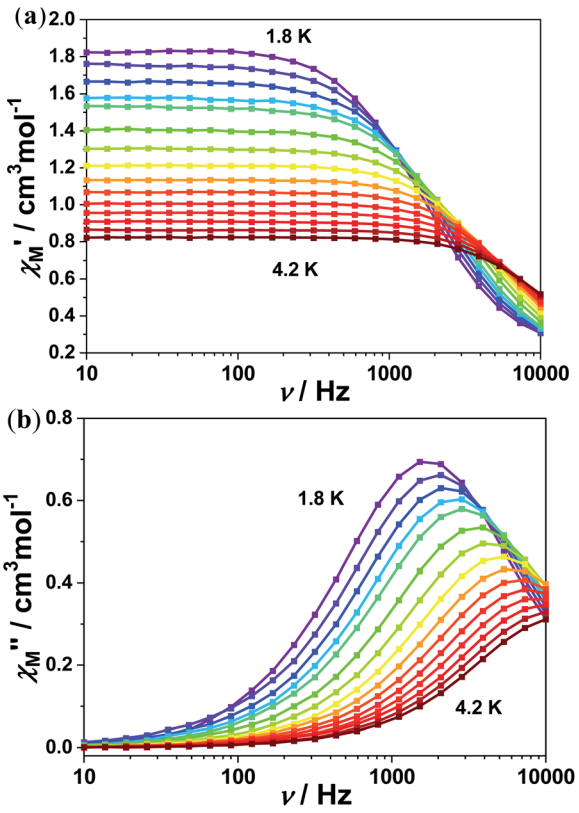

Fig. 3 Frequency-dependent (a) in-phase (χ') and (b) out-of phase (χ'') ac susceptibilities under 0.8 kOe dc fields for **1**.

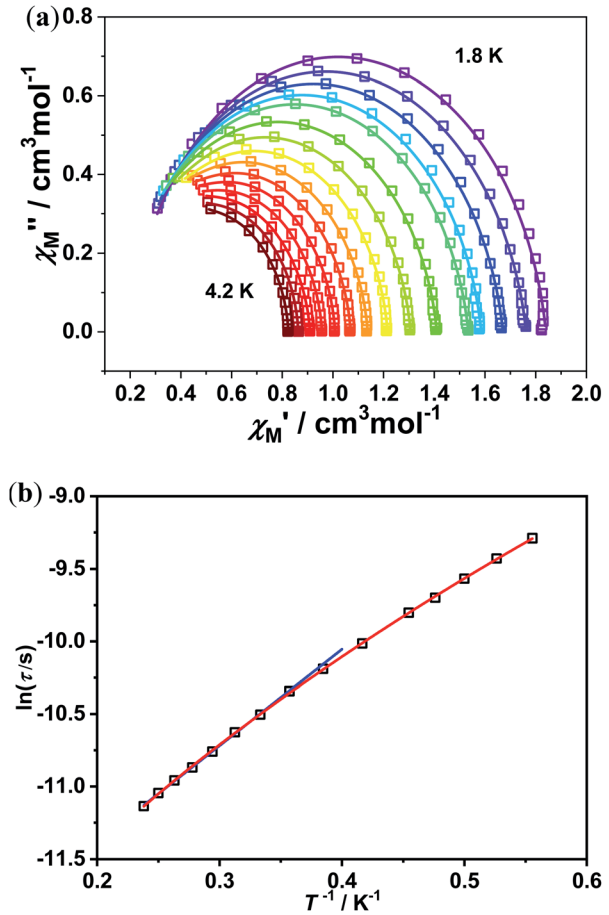

Fig. 4 (a) Cole–Cole curves of **1**. The solid lines stand for the best fit with Debye model. (b) A plot of ln(τ/s) *versus* T^{-1} with the solid line stands for linear fit to the Arrhenius equation (blue represent eqn (2), red represent eqn (3)).

process.[23] In the equation used, C represent the coefficient of the Raman process.

Since the multiple relaxation processes may exist in field-induced Co(II)-based SIMs, the general eqn (2) containing may not be suitable for precise analysis.[23] In the purpose to eliminate the deviation, four relaxation processes eqn (3) was employed for analysis, where C and n are the coefficient of the Raman process, U_{eff} represent for the energy barrier of Orbach process, k_B and T are the Boltzmann constant and temperature respectively. According to eqn (3), the effective energy barrier is $U_{eff} = 6.64$ K and $\tau_0 = 3.02 \times 10^{-6}$ s while $C = 1858.98$ K$^{-2.0067}$ s^{-1}, $n = 2.0067$, $U_{eff} = 6.32$ K and $\tau_0 = 6.24 \times 10^{-6}$ s for eqn (3).

$$\tau^{-1} = {\tau_0}^{-1} \exp(-U_{eff}/k_B T) \quad (2)$$

$$\tau^{-1} = CT^n + {\tau_0}^{-1} \exp(-U_{eff}/k_B T) \quad (3)$$

Conclusions

In summary, we herein report the syntheses, structure features, and magnetic properties of cobalt complex possessing two metal centres, forming a distorted trigonal antiprismatic geometry. The studied complex showed a field induced slow relaxation behaviour. The complex displayed an obvious peak of out-of-phase after 1000 Hz, indicating a powerful slow relaxation behaviour. The measured effective energy barrier is 6.32 K. According to previously reported, magnetic coupling is beneficial to reduce quantum tunnelling. This work highlights that the antiferromagnetic coupling however, did not amount to a great deal in inhibiting quantum tunnelling, as well as reducing slow relaxation behaviour. To sum up, the result reflected the importance of the ferromagnetic or antiferromagnetic couple for taking control of the suppress quantum tunnelling and may increase the effective energy barrier and blocking temperature. These study could offer some help in designing new excellent SMMs.

Conflicts of interest

There are no conflicts to declare.

Acknowledgements

We show thinks to Dr He for his kindly support to this study.

Notes and references

1 (*a*) M. L. Kirk, D. A. Shultz, D. E. Stasiw, D. Habel-Rodriguez, B. Stein and P. D. Boyle, *J. Am. Chem. Soc.*, 2013, **135**, 14713–14725; (*b*) R. Sessoli, D. Gatteschi, A. Caneschi and M. A. Novak, *Nature*, 1993, **365**, 141–143; (*c*) W. Wernsdorfer and R. Sessoli, *Science*, 1999, **284**, 133–135; (*d*) D. N. Woodruff, R. E. P. Winpenny and R. A. Layfield, *Chem. Rev.*, 2013, **113**, 5110–5148.

2 (*a*) F. Habib, I. Korobkov and M. Murugesu, *Dalton Trans.*, 2015, **44**, 6368–6373; (*b*) J. Li, Y. Han, F. Cao, R.-M. Wei, Y.-Q. Zhang and Y. Song, *Dalton Trans.*, 2016, **45**, 9279–9284.

3 N. Ishikawa, M. Sugita, T. Ishikawa, S.-y. Koshihara and Y. Kaizu, *J. Am. Chem. Soc.*, 2003, **125**, 8694–8695.

4 F. S. Guo, B. M. Day, Y. C. Chen, M. L. Tong, A. Mansikkamäki and R. A. Layfield, *Science*, 2018, **362**, 1400–1403.

5 (*a*) W. M. Wang, T. L. Han, Y. L. Shao, X. Y. Qiao, Z. L. Wu, Q. L. Wang, P. F. Shi, H. L. Gao and J. Z. Cui, *New J. Chem.*, 2018, **42**, 14949–14955; (*b*) W. M. Wang, X. M. Kang, H. Y. Shen, Z. L. Wu, H. L. Gao and J. Z. Cui, *Inorg. Chem. Front.*, 2018, **5**, 1876–1885.

6 (*a*) W. M. Wang, X. Z. Li, L. Zhang, J. L. Chen, J. H. Wang, Z. L. Wu and J. Z. Cui, *New J. Chem.*, 2019, **43**, 7419–7426; (*b*) W. M. Wang, Z. L. Wu, Y. X. Zhang, H. Y. Wei, H. L. Gao and J. Z. Cui, *Inorg. Chem. Front.*, 2018, **5**, 2346–2354.

7 G. A. Craig and M. Murrie, *Chem. Soc. Rev.*, 2015, **44**, 2135–2147.

8 J. Vallejo, A. Pascual-Álvarez, J. Cano, I. Castro, M. Julve, F. Lloret, J. Krzystek, G. DeMunno, D. Armentano, W. Wernsdorfer, R. Ruiz-García and E. Pardo, *Angew. Chem., Int. Ed.*, 2013, **52**, 14075–14079.

9 M. Ding, G. E. Cutsail III, D. Aravena, M. Amoza, M. Rouzières, P. Dechambenoit, Y. Losovyj, M. Pink, E. Ruiz, R. Clérac and J. M. Smith, *Chem. Sci.*, 2016, **7**, 6132–6140.

10 Y. F. Deng, T. Han, Z. Wang, Z. Ouyang, B. Yin, Z. Zheng, J. Krzystek and Y. Z. Zheng, *Chem. Commun.*, 2015, **51**, 17688–17691.

11 (*a*) J. M. Zadrozny, M. Atanasov, A. M. Bryan, C. Y. Lin, B. D. Rekken, P. P. Power, F. Neese and J. R. Long, *Chem. Sci.*, 2013, **4**, 125–138; (*b*) W. H. Harman, T. D. Harris, D. E. Freedman, H. Fong, A. Chang, J. D. Rinehart, A. Ozarowski, M. T. Sougrati, F. Grandjean, G. J. Long, J. R. Long and C. J. Chang, *J. Am. Chem. Soc.*, 2010, **132**, 18115–18126; (*c*) P. H. Lin, N. C. Smythe, S. I. Gorelsky, S. Maguire, N. J. Henson, I. Korobkov, B. L. Scott, J. C. Gordon, R. T. Baker and M. Murugesu, *J. Am. Chem. Soc.*, 2011, **133**, 15806–15809.

12 A. Eichhöfer, Y. Lan, V. Mereacre, T. Bodenstein and F. Weigend, *Inorg. Chem.*, 2014, **53**, 1962–1974.

13 K. E. R. Marriott, L. Bhaskaran, C. Wilson, M. Medarde, S. T. Ochsenbein, S. Hill and M. Murrie, *Chem. Sci.*, 2015, **6**, 6823–6828.

14 Y. S. Meng, Y. S. Qiao, M. W. Yang, J. Xiong, T. Liu, Y. Q. Zhang, S. D. Jiang, B. W. Wang and S. Gao, *Inorg. Chem. Front.*, 2020, **7**, 447–454.

15 (*a*) C. Y. Jin, X. L. Li, Z. L. Liu, A. Mansikkamäki and J. K. Tang, *Dalton Trans.*, 2020, **49**, 10477; (*b*) S. T. Liu, J. J. Lu, X. L. Li, Z. H. Zhu and J. K. Tang, *Dalton Trans.*, 2020, **49**, 12372.

16 (*a*) Z. B. Hu, Z. Y. Jing, M. M. Li, L. Yin, Y. D. Gao, F. Yu, T. P. Hu, Z. Wang and Y. Song, *Inorg. Chem.*, 2018, **57**, 10761–10767; (*b*) J. Zhang, J. Li, L. Yang, C. Yuan, Y. Q. Zhang and Y. Song, *Inorg. Chem.*, 2018, **57**, 3903–3912.

17 (*a*) G. M. Sheldrick, *Acta Crystallogr., Sect. A: Found. Crystallogr.*, 2008, **64**, 112–122; (*b*) G. M. Sheldrick, *Acta Crystallogr., Sect. A: Found. Crystallogr.*, 2015, **71**, 3–8.

18 G. M. Sheldrick, *SHELX-97*, University of Gottingen, 1997.

19 M. Murrie, *Chem. Soc. Rev.*, 2010, **39**, 1986–1995.

20 F. S. Ham, G. W. Ludwig, G. D. Watkins and H. H. Woodbury, *Phys. Rev. Lett.*, 1960, **5**, 468–470.

21 D. Gatteschi and R. Sessoli, *Angew. Chem., Int. Ed.*, 2003, **42**, 268–297.

22 K. S. Cole and R. H. Cole, *J. Chem. Phys.*, 1941, **9**, 341–352.

23 V. Chandrasekhar, A. Dey, A. J. Mota and E. Colacio, *Inorg. Chem.*, 2013, **52**, 4554–4561.